New results on the hadronic vacuum polarization contribution to the muon $g-2$

Michel Davier[1)]

Laboratoire de l'Accélérateur Linéaire, IN2P3/CNRS, Université Paris-Sud 11, Orsay 91898, France

Abstract Results on the lowest-order hadronic vacuum polarization contribution to the muon magnetic anomaly are presented. They are based on the latest published experimental data used as input to the dispersion integral. Thus recent results on $\tau \to \nu_\tau \pi\pi^0$ decays from Belle and on e^+e^- annihilation to $\pi^+\pi^-$ from *BABAR* and KLOE are included. The new data, together with improved isospin-breaking corrections for τ decays, result into a much better consistency among the different results. A discrepancy between the Standard Model prediction and the direct $g-2$ measurement is found at the level of 3σ.

Key words muon magnetic moment, vacuum polarization, electron-positron annihilation, tau decays, g-2

PACS 13.40Em, 13.60.Hb, 13.66.Bc, 13.66.Jn

1 Introduction

The Standard Model (SM) prediction of the anomalous magnetic moment of the muon, a_μ, is limited in precision by contributions from hadronic vacuum polarisation (HVP) loops. These contributions can be conveniently separated into a dominant lowest order ($a_\mu^{\rm had,LO}$) and higher order ($a_\mu^{\rm had,HO}$) parts. The lowest order term can be calculated with a combination of experimental cross section data involving e^+e^- annihilation to hadrons, and perturbative QCD. These are used to evaluate an energy-squared dispersion integral, ranging from the $\pi^0\gamma$ threshold to infinity. The integration kernel strongly emphasises the low-energy part of the spectrum, dominated by the $\pi\pi$ final state[2)]. When using e^+e^- data a deviation of more than 3σ was observed [1–3] between the SM prediction and the direct experimental value [4].

A former lack of precise e^+e^--annihilation data inspired the search for an alternative. It was found [5] in form of $\tau \to \nu_\tau +$hadrons spectral functions, transferred from the charged to the neutral state using isospin symmetry. During the last decade, new measurements of the $\pi\pi$ spectral function in e^+e^- annihilation with percent accuracy became available, superseding or complementing older and less precise data. With the increasing precision, which today is on a level with the τ data in that channel, systematic discrepancies in shape and normalisation of the spectral functions were observed between the two systems [6, 7]. It was found that, when computing the hadronic VP contribution to the muon magnetic anomaly using the τ instead of the e^+e^- data for the 2π and 4π channels, the observed deviation with the experimental value would reduce to less than 1σ [1]. Fig. 1 summarizes the comparison between theory and experiment by 2006-8 [1].

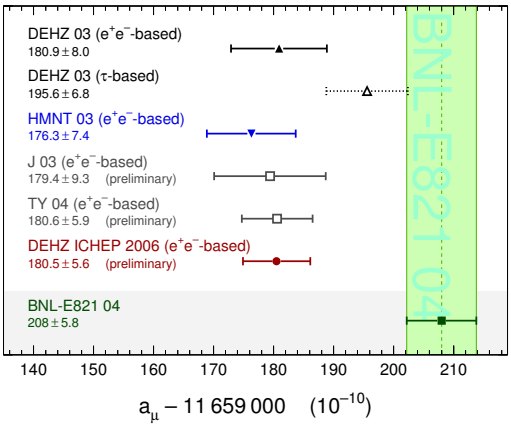

Fig. 1. Comparison of the predictions for the muon magnetic anomaly with the BNL measurement [4] in 2006, from (top to bottom) Refs. [1, 7–10].

Received 25 January 2010

1) E-mail: davier@lal.in2p3.fr

2) Throughout this paper, final state photon radiation is implied for hadronic final states

In this review I present the situation as of October 2009, taking advantage of very recent papers: (1) an updated analysis [11] using τ data, including high-statistics Belle results [12] and an improved treatment of isospin-breaking corrections (IB) [13]; (2) a *BABAR* measurement [14] of the ππ spectral function using the hard initial state radiation (ISR) method, benefiting from a large cancellation of systematic effects in the ratio $\pi\pi\gamma(\gamma)$ to $\mu\mu\gamma(\gamma)$ employed for the measurement; and (3) a global analysis [15] of all published e^+e^-data.

2 HVP and $g-2$

It is convenient to separate the Standard Model (SM) prediction for the anomalous magnetic moment of the muon into different contributions,

$$a_\mu^{\rm SM} = a_\mu^{\rm QED} + a_\mu^{\rm had} + a_\mu^{\rm weak} \ , \qquad (1)$$

with

$$a_\mu^{\rm had} = a_\mu^{\rm had,LO} + a_\mu^{\rm had,HO} + a_\mu^{\rm had,LBL} \ , \qquad (2)$$

and where $a_\mu^{\rm QED} = (11\,658\,471.810 \pm 0.016)\ 10^{-10}$ is the pure electromagnetic contribution [16], $a_\mu^{\rm had,LO}$ is the lowest-order HVP contribution, $a_\mu^{\rm had,HO} = (-9.79 \pm 0.08_{\rm exp} \pm 0.03_{\rm rad})\ 10^{-10}$ is the corresponding higher-order part [8, 17], and $a_\mu^{\rm weak} = (15.4 \pm 0.1 \pm 0.2)\ 10^{-10}$, where the first error is the hadronic uncertainty and the second is due to the Higgs mass range, accounts for corrections due to exchange of the weakly interacting bosons up to two loops [18]. For the light-by-light (LBL) scattering part, $a_\mu^{\rm had,LBL}$, we use the value $(10.5 \pm 2.6)\ 10^{-10}$ from the latest evaluation [19].

Owing to unitarity and to the analyticity of the vacuum-polarization function, the lowest order HVP contribution to a_μ can be computed through the dispersion integral [20]

$$a_\mu^{\rm had,LO} = \frac{\alpha^2}{3\pi^2} \int_{4m_\pi^2}^{\infty} {\rm d}s\, \frac{K(s)}{s} R^{(0)}(s) \ , \qquad (3)$$

where $K(s)$ is a well-known QED kernel, $\alpha = \alpha(s=0)$, and $R^{(0)}(s)$ denotes the ratio of the "bare" cross section for e^+e^- annihilation into hadrons to the point-like muon-pair cross section. The bare cross section is defined as the measured cross section corrected for initial-state radiation, electron-vertex loop contributions and vacuum-polarization effects in the photon propagator. However, photon radiation in the final state is included in the bare cross section defined here. The reason for using the bare (i.e., lowest order) cross section is that a full treatment of higher orders is anyhow needed at the level of a_μ, so that the use of the "dressed" cross section would entail the risk of double-counting some of the higher-order contributions.

The function $K(s) \sim 1/s$ in Eq. (3) gives a strong weight to the low-energy part of the integral. About 91% of the total contribution to $a_\mu^{\rm had,LO}$ is accumulated at centre-of-mass energies $\sqrt{s}$ below 1.8 GeV and 73% is covered by the ππ final state, which is dominated by the ρ(770) resonance.

3 Updated 2π analysis using τ data

3.1 Spectral functions in τ decays

The spectral function of the vector current decay $\tau \to {\rm X}^-\nu_\tau$ is related to the $e^+e^- \to {\rm X}^0$ cross section of the corresponding isovector final state $\rm X^0$,

$$\sigma_{\rm X^0}^{I=1}(s) = \frac{4\pi\alpha^2}{s} v_{1,\,{\rm X}^-}(s) \ , \qquad (4)$$

where s is the centre-of-mass energy-squared or equivalently the invariant mass-squared of the τ final state X, α is the electromagnetic fine structure constant, and $v_{1,\,{\rm X}^-}$ is the non-strange, isospin-one vector spectral function corrected for IB and given by

$$v_{1,\,{\rm X}^-}(s) \ = \ \frac{m_\tau^2}{6\,|V_{\rm ud}|^2} \frac{\mathcal{B}_{\rm X^-}}{\mathcal{B}_{\rm e}} \frac{1}{N_{\rm X}} \frac{{\rm d}N_{\rm X}}{{\rm d}s} \times \left(1 - \frac{s}{m_\tau^2}\right)^{-2} \left(1 + \frac{2s}{m_\tau^2}\right)^{-1} \frac{R_{\rm IB}(s)}{S_{\rm EW}} , \qquad (5)$$

with

$$R_{\rm IB}(s) = \frac{{\rm FSR}(s)}{G_{\rm EM}(s)} \frac{\beta_0^3(s)}{\beta_-^3(s)} \left| \frac{F_0(s)}{F_-(s)} \right|^2 . \qquad (6)$$

In Eq. (5), $(1/N_{\rm X}){\rm d}N_{\rm X}/{\rm d}s$ is the normalised invariant mass spectrum of the hadronic final state, and $\mathcal{B}_{\rm X^-}$ denotes the branching fraction of $\tau \to \nu_\tau {\rm X}^-$. We use for the τ mass the value $m_\tau = (1776.84 \pm 0.17)$ MeV [21], and for the CKM matrix element $|V_{\rm ud}| = 0.97418 \pm 0.00019$ [22], which assumes CKM unitarity. For the electron branching fraction we use $\mathcal{B}_{\rm e} = (17.818 \pm 0.032)\%$, obtained [23] supposing lepton universality. Short-distance electroweak radiative effects lead to the correction $S_{\rm EW} = 1.0235 \pm 0.0003$ [6, 24–26]. All the s-dependent IB corrections are included in $R_{\rm IB}$, which have been worked out in the 2π channel: ${\rm FSR}(s)$ refers to the final state radiative corrections [27], and $G_{\rm EM}(s)$ denotes the long-distance radiative corrections of order α to the photon inclusive τ spectrum, computing the virtual and real photonic corrections using chiral resonance [28] or vector dominance [29].

3.2 Improved IB corrections

As the physics of IB is described elsewhere [13] I only concentrate here on the major difference between

the previous analysis [6, 7] and the new one [11]. In Eq. (6) the ratio of the electromagnetic $F_0(s)$ and weak $F_-(s)$ form factors depends on the charged and neutral ρ parameters, as well as ρ-ω interference. While a small mass difference (of the order of 1 MeV) makes only a small effect on the dispersion integral because of its bipolar nature, a difference in the width can lead to a significant correction. Such a difference is expected from radiative $\rho \to \pi\pi\gamma$ decays which have been evaluated in a scalar-QED vector-dominance model [30]. The result is markedly different from the estimate made previously using only the hard radiation part [31].

One could question the validity of using point-like pions in the calculation of radiative decays. However several experimental tests support this assumption in $e^+e^- \to \pi^+\pi^-\gamma(\gamma)$ for the same mass range: lowest-order FSR with KLOE [32], additional FSR with *BABAR* [14].

The new IB corrections are listed in Table 1.

3.3 Consistency of τ spectral functions

All published τ 2π spectral functions are normalised to the world-average branching ratio. The shape of their mass dependence can be compared by looking at the relative difference between each spectral function and the combined one, locally averaging the data from ALEPH [33], CLEO [34], OPAL [35], and Belle [12] (Fig. 2).

Table 1. Contributions to $a_\mu^{\rm had,LO}$ $[\pi\pi,\tau]$ from the isospin-breaking corrections. Corrections shown in two separate columns correspond to the Gounaris-Sakurai (GS) and Kühn-Santamaria (KS) form factor parametrisations, respectively.

source	$\Delta\, a_\mu^{\rm had,LO}$ $[\pi\pi,\tau]$ (10^{-10})	
	GS Model	KS Model
$S_{\rm EW}$	-12.21 ± 0.15	
$G_{\rm EM}$	-1.92 ± 0.90	
FSR	$+4.67\pm0.47$	
ρ-ω interference	$+2.80\pm0.19$	$+2.80\pm0.15$
$m_{\pi^\pm}-m_{\pi^0}$ (σ)	-7.88	
$m_{\pi^\pm}-m_{\pi^0}$ (Γ_ρ)	$+4.09$	$+4.02$
$m_{\rho^\pm}-m_{\rho^0_{\rm bare}}$	$+0.20^{+0.27}_{-0.19}$	$+0.11^{+0.19}_{-0.11}$
ππγ, EM decays	-5.91 ± 0.59	-6.39 ± 0.64
total	-16.07 ± 0.59	-16.70 ± 0.64
	-16.07 ± 1.85	

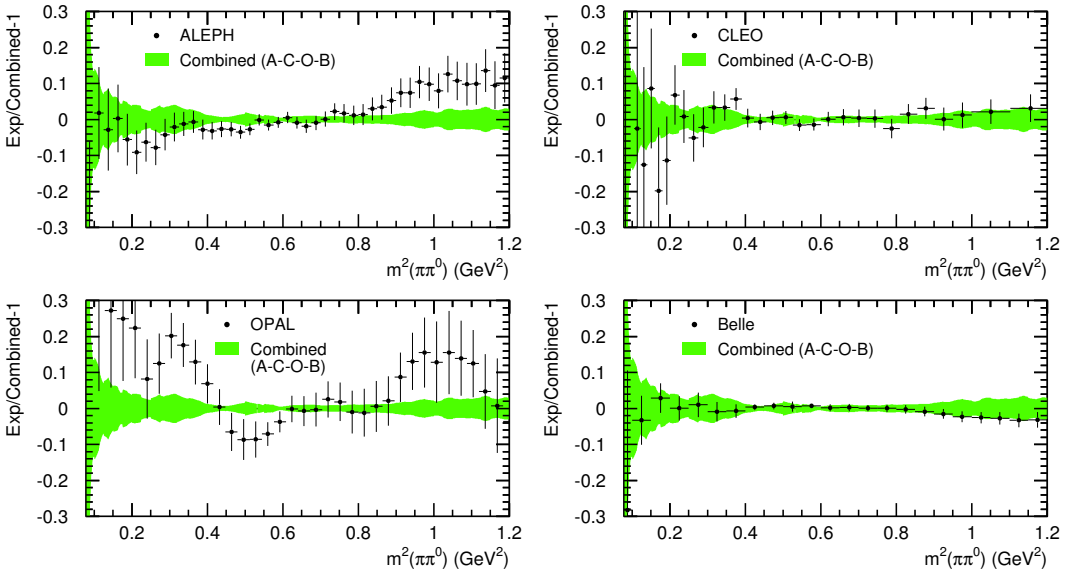

Fig. 2. Relative comparison between the $\tau \to \nu_\tau\pi\pi^0$ spectral functions from ALEPH, CLEO, OPAL, Belle (data points) and their combined result (shaded band).

Since the world-average branching ratio is dominated by the ALEPH result, it is interesting to test the consistency between the absolute spectra, i.e. when each spectrum is normalised to the branching ratio measured by the same experiment. Fig. 3 shows a very good agreement between the full dispersion integrals with comparable uncertainties. Thus the τ experiments yield consistent absolute results. The average value and its error are rather insensitive to the branching ratio choice, although it is not true at the level of individual experiments. In particular the Belle result reaches its best precision only when the

world-average is used.

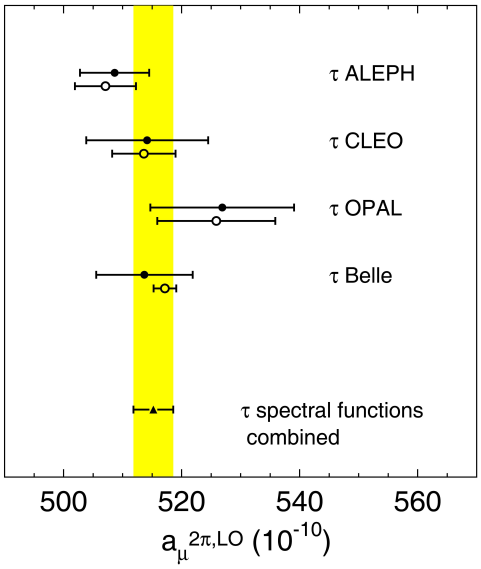

Fig. 3. Comparison of the $a_\mu^{had,LO}[\pi\pi]$ values for different τ experiments using their own $\tau \to \nu_\tau \pi\pi^0$ branching ratios (closed circles) or the world-average (open circles).

3.4 Comparison to e^+e^- Data

Figure 4 shows the relative difference between the ee and the IB-corrected τ spectral functions versus s. The relative normalisation is consistent within the respective errors and the shape is found in better agreement than before [7], despite a remaining deviation above the ρ-mass-squared. The discrepancy with the KLOE data, although reduced, persists.

As the g-2 dispersion relation involves an integral over the hadronic spectral function, it is interesting to consider the result with another kernel. By integrating the e^+e^- data weighted by the τ matrix element C_τ, and correcting for IB, one obtains the branching ratio $B^{CVC}_{\pi\pi^0}$ which can be directly compared to the measurements. Indeed,

$$B^{CVC}_{\pi\pi^0} = \frac{3}{2}\frac{S_{EW}B_e|V_{ud}|^2}{\pi\alpha^2 m_\tau^2}\int_{4m_\pi^2}^{m_\tau^2} ds\, s\, \frac{\sigma_{\pi^+\pi^-}}{R_{IB}} C_\tau, \quad (7)$$

$$C_\tau = \left(1-\frac{s}{m_\tau^2}\right)^2\left(1+\frac{2s}{m_\tau^2}\right). \quad (8)$$

The results for $B^{CVC}_{\pi\pi^0}$ from e^+e^- experiments are compared to the direct measurements in Fig. 5 The average, $(24.78 \pm 0.17_{exp} \pm 0.22_{IB})\%$, differ from the average τ branching ratio, $(25.42\pm0.10)\%$, by $(0.64\pm 0.10_\tau\pm0.17_{ee}\pm0.22_{IB})\%$ to be compared to an applied IB correction of $(+0.69)\%$. The discrepancy of about 2σ is significantly reduced from the previous analysis [1] (4.5σ). It should be emphasized that the observed increased deviation above the ρ mass between ee and τ spectral functions, essentially driven by the KLOE data, plays a more significant role in the $B^{CVC}_{\pi\pi^0}$ integral, rather than in the a_μ integral with its much steeper kernel. So we expect a better consistency for $g-2$.

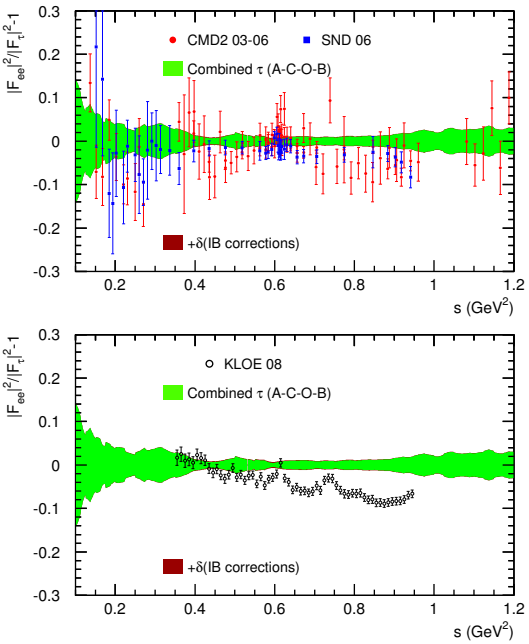

Fig. 4. Relative comparison between ee and τ spectral functions, expressed in terms of the difference between neutral and charged pion form factors. Isospin-breaking corrections are applied to τ data with the corresponding uncertainties included in the error band.

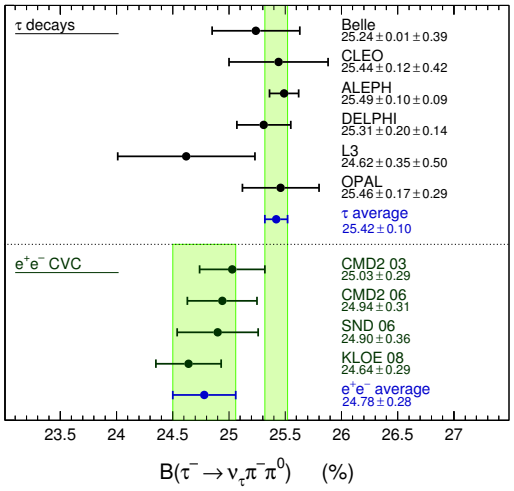

Fig. 5. The measured branching fractions for $\tau \to \nu_\tau \pi\pi^0$ (references in [11]) compared to the predictions from the $e^+e^- \to \pi^+\pi^-$ spectral functions, applying the IB corrections. For the ee results, only the data from the indicated experiments in the 0.63–0.958 GeV range are used, and the combined ee data elsewhere. Vertical bands indicate average values.

4 Updated 2π analysis using e^+e^- including *BABAR*

4.1 The data

Recent precision data, where all required radiative corrections have been applied by the experiments, stem from the CMD-2 [37] and SND [38] experiments at the VEPP-2M collider. They achieve comparable statistical errors, and energy-dependent systematic uncertainties down to 0.8% and 1.3%, respectively.

These measurements have been complemented by results from KLOE [39] at DAΦNE running at the φ resonance centre-of-mass energy. KLOE applied for the first time the ISR technique to precisely determine the ππ cross section between 0.592 and 0.975 GeV. The high statistics of the analysed data sample yields a 0.2% relative statistical error on the ππ contribution to $a_\mu^{\rm had,LO}$. KLOE normalises the πγ cross section taking the absolute ISR radiator function from Monte Carlo simulation (Ref. [40] and references therein). The systematic error assigned to this correction varies between 0.5% and 0.9% (closer to the φ peak). The total assigned systematic error lies between 0.8% and 1.2%.

In a recent publication [14] the *BABAR* Collaboration reported measurements of the processes $ee \to \pi\pi\gamma, \mu\mu\gamma$ using the ISR method at 10.6 GeV centre-of-mass energy. The detection of the hard ISR photon allows *BABAR* to cover a large energy range from threshold up to 3 GeV for the two processes. The ππ(γ) cross section is obtained from the πγ(γ) to μμγ(γ) ratio, so that the ISR radiation function cancels, as well as additional ISR radiative effects. Since additional FSR photons are also detected, there is no additional uncertainty from radiative corrections at NLO level. Experimental systematic uncertainties are kept to 0.5% in the ρ peak region (0.6–0.9 GeV), increasing to 1% outside.

4.2 Combining cross section data

The details of the combination procedure are given in Ref. [15]. The requirements for averaging and integrating cross section data are: (i) properly propagate all the uncertainties in the data to the final integral error, (ii) minimise biases, i.e., reproduce the true integral as closely as possible in average and measure the remaining systematic error, and (iii) minimise the integral error after averaging while respecting the two previous requirements. The first item practically requires the use of pseudo-Monte Carlo (MC) simulation, which needs to be a faithful representation of the measurement ensemble and to contain the full data treatment chain (interpolation, averaging, integration). The second item requires a flexible data interpolation method and a realistic truth model used to test the accuracy of the integral computation with pseudo-MC experiments. Finally, the third item requires optimal data averaging taking into account all known correlations to minimise the spread in the integral measured from the pseudo-MC sample.

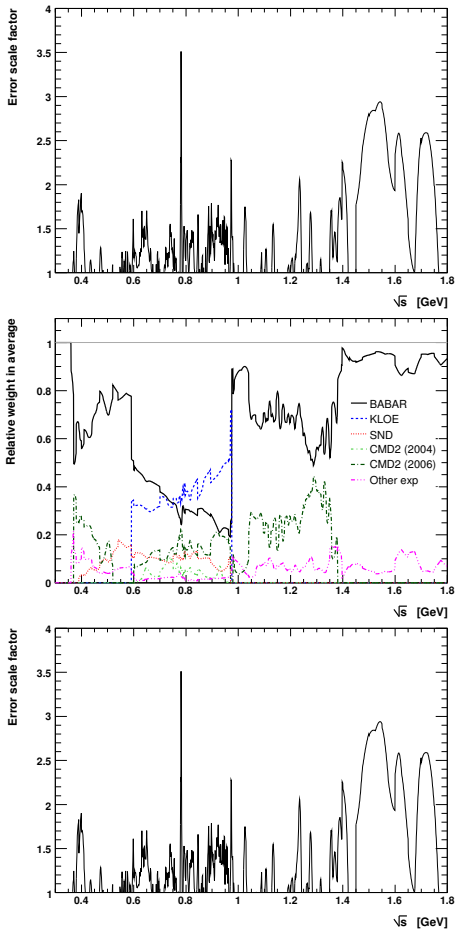

Fig. 6. (color online) Top: Error rescaling factor accounting for inconsistencies among experiments versus $\sqrt{s}$. Middle: Relative averaging weights for each experiment versus $\sqrt{s}$. Bottom: Contribution to the dispersion integral for the combined ee data obtained by multiplying the ππ cross section by the kernel function K(s) (solid line). The dashed (red) curve belonging to the right axis shows the corresponding error contribution, where statistical and systematic errors have been added in quadrature.

The combination and integration of the $ee \to \pi\pi$ cross section data is performed using the newly developed software package HVPTools [36]. It transforms the bare cross section data and associated sta-

tistical and systematic covariance matrices into fine-grained energy bins, taking into account to our best knowledge the correlations within each experiment as well as between the experiments (such as uncertainties in radiative corrections). The covariance matrices are obtained by assuming common systematic error sources to be fully correlated. To these matrices are added statistical covariances, present for example in binned measurements as provided by KLOE, *BABAR* or the τ data, which are subject to bin-to-bin migration that has been unfolded by the experiments, thus introducing correlations. The interpolation between adjacent measurements of a given experiment uses second-order polynomials, which is an improvement with respect to the previously applied trapezoidal rule. In the case of binned data, the interpolation function within a bin is renormalised to keep the integral in that bin invariant after the interpolation. The final interpolation function per experiment within its applicable energy domain is discretised into small (1 MeV) bins for the purpose of averaging and numerical integration.

The averaging of the interpolated measurements from different experiments contributing to a given energy bin is the most delicate step in the analysis chain. Correlations between measurements and experiments must be taken into account. Moreover, the experiments have different measurement densities or bin widths within a given energy interval and one must avoid that missing information in case of a lower measurement density is substituted by extrapolated information from the polynomial interpolation. To derive proper weights given to each experiment, wider averaging regions are defined to ensure that all locally available experiments contribute to the averaging region, and that in case of binned measurements at least one full bin is contained in it. The averaging regions are used to compute weights for each experiment, which are applied in the bin-wise average of the original finely binned interpolation functions. If the χ^2 value exceeds the number of degrees of freedom ($n_{\rm dof}$), the error in the averaged bin is rescaled by $\sqrt{\chi^2/n_{\rm dof}}$ to account for inconsistencies. Fig. 6 shows the distributions in $\sqrt{s}$ of the error recaling factor, the relative weights for each experiment, and the contribution to the dispersion integral, as well as its error. It is seen that *BABAR* dominates the averaging up to the ρ peak and above 0.95 GeV, while KLOE has a larger weight in-between owing to the steep behaviour of the radiator function when approaching 1 GeV. The uncertainty in the integral is dominated by the measurements below 0.8 GeV.

The consistent propagation of all errors into the evaluation of $a_\mu^{\rm had,LO}$ is ensured by generating large samples of pseudo experiments, representing the full list of available measurements and taking into account all known correlations. For each generated set of pseudo measurements, the identical interpolation

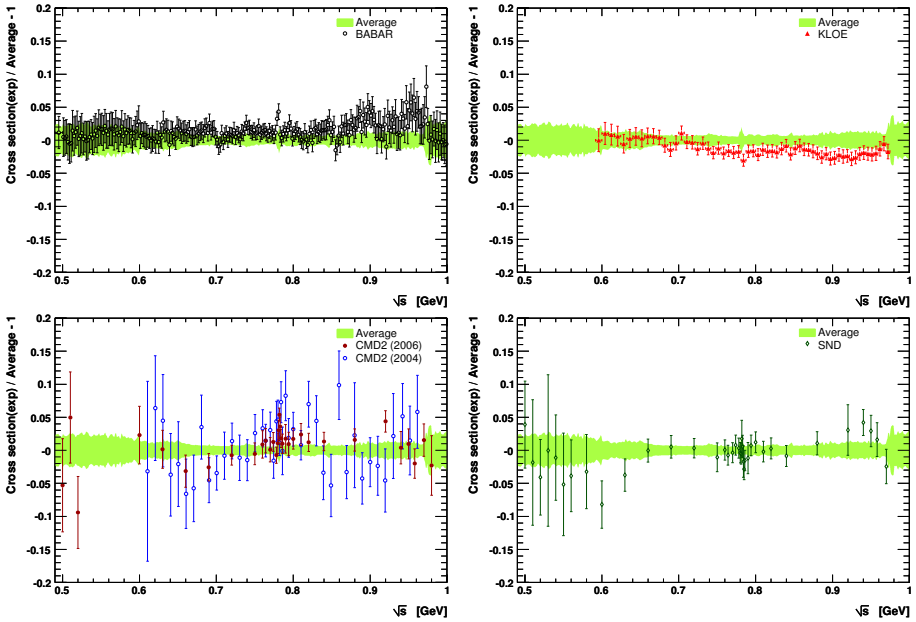

Fig. 7. Relative cross section comparison between individual experiments (symbols) and the HVPTools average (shaded band) computed from all measurements considered. Shown are *BABAR* (top left), KLOE (top right), CMD-2 (bottom left) and SND (bottom right).

and averaging treatment leading to the computation of Eq. (3) as for real data is performed, hence resulting in a probability density distribution for $a_\mu^{\rm had,LO}[\pi\pi]$, the mean and RMS of which define the 1σ allowed interval.

The fidelity of the full analysis chain (polynomial interpolation, averaging, integration) has been tested with toy models, using as truth representation a Gounaris-Sakurai vector-meson resonance model faithfully describing the $\pi\pi$ data. Negligible biases below 0.1 (10^{-10} units) are found, increasing to 0.5 (1.2 without the high-density *BABAR* data) when using the trapezoidal rule for interpolation instead of second order polynomials.

The relative differences between *BABAR* KLOE, CMD-2, SND, and their average are given in Fig. 7. Fair agreement is observed, though with a tendency to larger (smaller) cross sections above ∼0.8 GeV for *BABAR* (KLOE). These inconsistencies (among others) lead to the error rescaling shown in Fig. 6.

4.3 Results for $a_\mu^{\rm had,LO}[\pi\pi]$

A compilation of results for $a_\mu^{\rm had,LO}[\pi\pi]$ for the various sets of experiments and energy regions is given in Table 2. The inclusion of the new *BABAR* data significantly increases the central value of the integral, without however providing a large error reduction, because of the incompatibility between mainly *BABAR* and KLOE, causing an increase of the combined error. In the energy interval between 0.63 and 0.958 GeV, the discrepancy between the $a_\mu^{\rm had,LO}[\pi\pi]$ evaluations from KLOE and *BABAR* amounts to 2.0σ.

Table 2. Evaluated $a_\mu^{\rm had,LO}[\pi\pi]$ contributions from the ee data for different energy intervals and experiments. Where two errors are given, the first is statistical and the second systematic. The last value in parentheses is the total error). Also given is the τ-based result.

$\sqrt{s}$/GeV	Exp.	$a_\mu^{\rm had,LO}[\pi\pi]$ (10^{-10})
$2m_{\pi^\pm}-.3$	ee fit	0.55 ± 0.01
$0.30-0.63$	Comb. ee	$132.6\pm0.8\pm1.0$ (1.3)
$0.63-0.958$	CMD2 03	$361.8\pm2.4\pm2.1$ (3.2)
	CMD2 06	$360.2\pm1.8\pm2.8$ (3.3)
	SND 06	$360.7\pm1.4\pm4.7$ (4.9)
	KLOE 08	$356.8\pm0.4\pm3.1$ (3.1)
	BABAR	$365.2\pm1.9\pm1.9$ (2.7)
	Comb. ee	$360.8\pm0.9\pm1.8$ (2.0)
$0.958-1.8$	Comb. ee	$14.4\pm0.1\pm0.1$ (0.2)
total	Comb. ee	$508.4\pm1.3\pm2.6$ (2.9)
total	Comb. τ	$515.2\pm2.0\pm2.7$ (3.4)

Since *BABAR* is the only experiment covering the entire energy region between $2m_\pi$ and 1.8 GeV, it can provide its own evaluation [14] of $a_\mu^{\rm had,LO}[\pi\pi]$, $514.1\pm2.2_{\rm stat}\pm3.1_{\rm syst}$ [1)].

5 Multihadronic contributions

We also reevaluate the $e^+e^-\to\pi^+\pi^-2\pi^0$ contribution to $a_\mu^{\rm had,LO}$. It is found that the CMD-2 data used previously have been superseded by modified or more recent, but yet unpublished data [41], recovering agreement with the published SND cross sections [42].

Since the new data are unavailable, we discard the obsolete CMD-2 data from the $\pi\pi2\pi^0$ average, finding $a_\mu^{\rm had,LO}[\pi\pi2\pi^0]=17.6\pm0.4_{\rm stat}\pm1.7_{\rm syst}$ (compared to $17.0\pm0.4_{\rm stat}\pm1.6_{\rm syst}$ when including the obsolete CMD-2 data). The corresponding cross section measurements and HVPTools average are shown in Fig. 8. From the still preliminary *BABAR* results [43] it is clear that the region above 1.4 GeV is still underestimated at the present state, as corroborated by τ data [6].

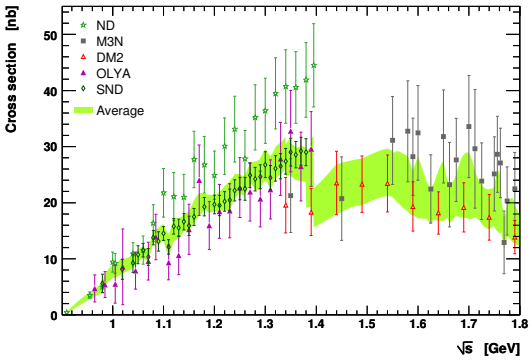

Fig. 8. Cross section measurements for $e^+e^-\to\pi^+\pi^-2\pi^0$ used in the calculation of $a_\mu^{\rm had,LO}[\pi\pi2\pi^0]$. The shaded band depicts the HVPTools interpolated average within 1σ errors. The individual measurements are referenced in Ref. [6].

6 Results and comparison to experiment

Adding to the ee-based $a_\mu^{\rm had,LO}[\pi\pi]$ and $a_\mu^{\rm had,LO}[\pi\pi2\pi^0]$ results the remaining exclusive multihadron channels as well as perturbative QCD [1], we find for the complete lowest-order hadronic term

$$a_\mu^{\rm had,LO}\ [\rm ee] = 695.5\pm4.0_{\rm exp}\pm0.7_{\rm QCD}\ (4.1_{\rm tot}). \quad (9)$$

It is noticeable that the error from the $\pi\pi$ channel now equals the one from all other contributions to $a_\mu^{\rm had,LO}$.

1) When not specified, the a_μ values are given in units of 10^{-10}.

Adding further the other contributions (given in Section 2), we obtain the Standard Model prediction (still in 10^{-10} units)

$$a_\mu^{\rm SM}\ [\rm ee] = 11\,659\,183.4 \pm 4.1 \pm 2.6 \pm 0.2\ (4.9_{\rm tot}),\quad (10)$$

where the errors have been split into lowest and higher-order hadronic, and other contributions, respectively. The $a_\mu^{\rm SM}$ [ee] value deviates from the experimental average [4], $a_\mu^{\rm exp} = 11\,659\,208.9 \pm 5.4 \pm 3.3$[1)], by 25.5 ± 8.0 (3.2σ). For comparison the difference obtained with the updated τ analysis is 15.7 ± 8.2 (1.9σ).

A compilation of recent SM predictions for a_μ compared with the experimental result is given in Fig. 9. The *BABAR* results are not yet contained in previous evaluations. The result by HMNT [2] contains older KLOE data [45], which have been superseded by more recent results [39] leading to a slightly larger value for $a_\mu^{\rm had,LO}$.

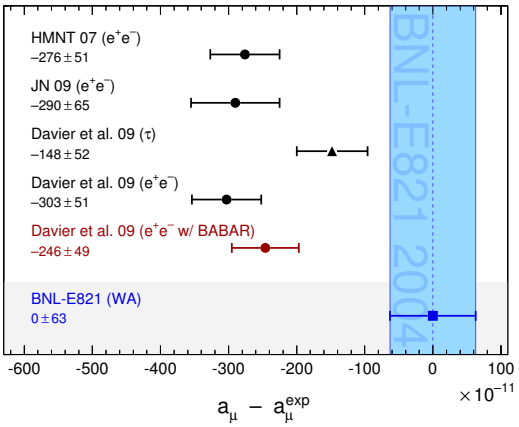

Fig. 9. Compilation of recent results for $a_\mu^{\rm SM}$, subtracted by the central value of the experimental average [4]. The shaded vertical band indicates the experimental error. The SM predictions are taken from: HMNT 07 [2], JN 09 [46], Davier et al. 09 [11] (τ-based and ee before *BABAR*), and the ee-based value [15] including *BABAR*.

7 Conclusions: discussion and perpectives

The following concluding remarks can be made:

1) The first point to emphasize is the better consistency between the ee and τ analyses, resulting from the improved IB corrections and the *BABAR* results. There is still a difference of $(6.8 \pm 2.9_{\rm ee} \pm 3.4_\tau)$ (1.5σ) in the $\pi\pi$ channel, but it can be considered as reasonable. The discrepancy was 2.9σ before, reduced to 2.4σ after the τ update. The other major difference affecting the two estimates is in the $2\pi 2\pi^0$ channel, $(3.8 \pm 1.7_{\rm ee} \pm 1.4_\tau)$ (1.7σ). For this case we have seen that a better measurement with e^+e^- will likely move the ee result closer to the τ value.

2) The internal consistency of the ee $\to \pi\pi$ data is only fair, as a discrepancy is observed between the *BABAR* and KLOE results, which is increasing with energy. The difference on the ρ peak, about 3% (beyond the respective systematic errors of 0.5% and 1.1%), is the most damaging for the dispersion integral. Here CMD-2 agrees well with *BABAR*, while SND lies between *BABAR* and KLOE. However, the accuracy of both CMD-2 and SND is not enough to resolve the issue.

3) While the *BABAR* measurement is explicitly done at NLO (including one additional ISR or FSR photon), it is insensitive to the Monte Carlo NLO generation. The situation is different for KLOE which relies on Phokhara for the ISR radiation function. Using the ISR process ee $\to \mu\mu$ *BABAR* has been able to verify that Phokhara provides the right answer to an accuracy of 1.1%, however in a kinematic region (very hard ISR photons, $x = 1 - s/s_0 > 0.9$, where s_0 is the square of the ee CM energy) far from that of KLOE ($0.09 < x < 0.66$). A measurement of the muon ISR process by KLOE has been considered since some time and would be of considerable help to validate their approach.

4) Although the accuracy of the *BABAR* results is similar to that of the combined previous ee experiments, the gain in precision that could have been hoped for was not realised because of the remaining discrepancy, essentially with KLOE.

5) All approaches now yield a deviation from the direct measurement, however at different levels depending on what $\pi\pi$ input data are used: 2.4σ with *BABAR* alone, 3.2σ with all ee data, 3.7σ with ee not including *BABAR*, 2.9σ with ee not including KLOE, and 1.9σ with τ alone.

6) Considering these results one can say there is some evidence for a deviation at the 3σ level. The significance is still not enough to establish a breakdown of the Standard Model in the muon $g-2$, i.e. a contribution from new physics. However it is a quantitative and very valuable information which will help to constrain the new physics, if it is found at the LHC.

1)The $g-2$ measurement is obtained from the ratio of two frequencies and needs as input the ratio of the muon to the proton magnetic moments. The latter ratio is derived from muonium hyperfine splitting, and its value has been updated [44] after the E-821 publication. The new value produces a shift of $+0.92\ 10^{-10}$ of the a_μ value.

This is the present situation. It should and will evolve as new results and new initiatives are taking place:

7) The hadronic spectral functions will continue to be refined as new results are expected from *BABAR* in the multihadronic channels, from KLOE ($\pi\pi$) with improved approaches (preliminary results are already available for the large-angle ISR analysis [32]), and from the upgraded CMD-3 and SND detectors at the higher-energy VEPP-2000 collider [47].

8) The theory error is still dominated by the uncertainty on the HVP contribution $(4.1)^{1)}$, but it is now close to that of the hadronic LBL part $(2.6)^{1)}$. Since the latter contribution is unlikely to be known more precisely in the short-term it will eventually be the theory show-stopper.

9) But the real limitation at the moment is the $g-2$ measurement itself. The uncertainty reached by E-821 is 6.3, larger than the full theory error (4.9). It is therefore mandatory to pursue these measurements in order to reach higher precision. The factor 20 in precision obtained at BNL over the pioneering measurements performed at CERN has permitted to reach the electroweak scale in this process. Another factor of 4, as anticipated by the new proposal [49] submitted to Fermilab, or with the JPARC project [50], will definitely provide quantitative information as we move into the new physics territory.

I would like to thank A. Höcker, B. Malaescu, G. López Castro, X.H. Mo, G. Toledo Sánchez, P. Wang, C.Z. Yuan, and Z. Zhang for our fruitful collaboration, and C.Z. Yuan and his colleagues for running a perfect workshop.

References

1 Davier M. Nucl. Phys. B (Proc. Suppl.), 2007, **169**: 288
2 Hagiwara K, Martin A D, Nomura D, Teubner T. Phys. Lett. B, 2007, **649**: 173
3 Jegerlehner F. Nucl. Phys. B (Proc. Suppl.), 2008, **181**: 26
4 Bennett G W et al. Phys. Rev. D, 2006, **73**: 072003
5 Alemany R, Davier M, Hoecker A. Eur. Phys. J. C, 1998, **2**: 123
6 Davier M, Eidelman S, Hoecker A, ZHANG Z. Eur. Phys. J. C, 2003, **27**: 497
7 Davier M, Eidelman S, Hoecker A, ZHANG Z. Eur. Phys. J. C, 2003, **31**: 503
8 Hagiwara K, Martin A D, Nomura D, Teubner T. Phys. Lett. B, 2003, **557**: 69
9 de Troconiz J F, Yndurain F J. hep-ph/0402285
10 Jegerlehner F. hep-ph/0312372
11 Davier M, Höcker A, Malaescu B, López Castro G, MO X H, Toledo Sánchez G, WANG P, YUAN C Z, ZHANG Z. arXiv:0906.5443, to appear in Eur. Phys. J. C.
12 Belle collaboration, Fujikawa M et al. Phys. Rev. D, 2008, **78**: 072006
13 López Castro G. these proceedings and references therein
14 *BABAR* collaboration, Aubert B et al. arXiv:0908.3589, Phys. Rev. Lett., 2009, **103**: 231801
15 Davier M, Höcker A, Malaescu B, YUAN C Z, ZHANG Z. arXiv:0908.4300, to appear in Eur. Phys. J. C
16 Kinoshita T, Nio M. Phys. Rev. D, 2006, **73**: 013003
17 Krause B. Phys. Lett. B, 1997, **390**: 392
18 Jackiw R, Weinberg S. Phys. Rev. D, 1972, **5**: 2396; Czarnecki A et al. Phys. Rev. D, 2003, **67**: 073006
19 Prades J, de Rafael E, Vainshtein A. arXiv:0901.0306
20 Gourdin M, de Rafael E. Nucl. Phys. B, 1969, **10**: 667; Brodsky S J, de Rafael E. Phys. Rev.,1968, **168**: 1620
21 Particle Data Group, Amsler C et al. Phys. Lett. B, 2008, **667**: 1
22 CKMfitter Group, Charles J et al. Eur. Phys. J. C, 2005, **41**: 1; updates from http://ckmfitter.in2p3.fr
23 Davier M, Hoecker A, Zhang Z. Rev. Mod. Phys., 2006, **78**: 1043
24 Sirlin A. Rev. Mod. Phys., 1978, **50**: 573 [Erratum-ibid.,1978, **50**: 905]; Marciano W, Sirlin A. Phys. Rev. Lett., 1988, **61**: 1815; Sirlin A. Nucl. Phys. B, 1982, **196**: 83
25 Braaten E, LI C S. Phys. Rev. D, 1988, **42**: 3888
26 Erler J. Rev. Mex. Fis., 2004, **50**: 200
27 Schwinger J S. Particles, Sources and Fields, Vol. 3, Reading, Massachusetts, 1989; Drees M, Hikasa K. Phys. Lett. B, 1990, **252**: 127
28 Cirigliano V, Ecker G, Neufeld H. Phys. Lett. B, 2001, **513**: 361; JHEP, 2002, **0208**: 002
29 Flores-Tlalpa A, Flores-Baez F, Lopez Castro G, Toledo Sanchez G. Phys. Rev. D, 2006, **74**: 071301; Nucl. Phys. Proc. Suppl., 2007, **169**: 250
30 Flores-Baez F, Lopez Castro G, Toledo Sanchez G. Phys. Rev. D, 2007, **76**: 096010
31 Singer P. Phys. Rev., 1963, **130**: 2441 1967, **161**: 1694
32 Müller S. these proceedings.
33 ALEPH Collaboration, Schael S et al. Phys. Rep., 2005, **421**: 191
34 CLEO Collaboration, Anderson S et al. Phys. Rev. D, 2000, **61**: 112002
35 OPAL collaboration, Ackerstaff K et al. Eur. Phys. J. C, 1999, **7**: 571
36 The HVPTools source code and database can be made publicly available by contacting the authors of Ref. [15]
37 CMD-2 collaboration, Akhmetshin R R et al. Phys. Lett. B, 2004, **578**: 285; CMD-2 collaboration, Aulchenko V M et al. JETP Lett., 2005, **82**: 743; CMD-2 collaboration, Akhmetshin R R et al. JETP Lett., 2006, **84**: 413; CMD-2 collaboration, Akhmetshin R R et al. Phys. Lett. B, 2007, **648**: 28
38 SND collaboration, Achasov M N et al. JETP Lett., 2006, **103**: 380
39 KLOE collaboration, Ambrosino F et al. Phys. Lett. B, 2009, **670**: 285
40 Czyż H, Grzelińska A, Kühn J H. Phys. Rev. D, 2007, **75**: 074026

1) The estimate given in Ref. [48] is larger (40).

41 Logashenko I B. Nucl. Phys. B (Proc. Suppl.), 2006, **162**: 13
42 SND collaboration, Achasov M N et al. Budker INP 2001-34, Novosibirsk, 2001
43 Solodov E P. these proceedings
44 Mohr P J, Taylor B J, Newell D B. Rev. Mod. Phys., 2008, **80**: 633
45 KLOE collaboration, Aloisio F et al. Phys. Lett. B, 2005, **606**: 12
46 Jegerlehner F, Nyffeler A. Phys. Rept., 2009, **477**: 1
47 Logashenko I B. these proceedings
48 Nyffeler A. these proceedings
49 Roberts B L. these proceedings
50 Mibe T. these proceedings